

Copy 222  
RM E53H25

NACA RM E53H25

TECH LIBRARY KAFB, NM  
0143278

NACA

# RESEARCH MEMORANDUM

JET EFFECTS ON FLOW OVER AFTERBODIES IN  
SUPERSONIC STREAM

By Edgar M. Cortright, Jr., and Fred D. Kochendorfer

Lewis Flight Propulsion Laboratory  
Cleveland, Ohio

Classification cancelled (or changed to *Unclassified*)

By Authority of *NASA Tech. Pub. Announcement #1*  
(OFFICER AUTHORIZED TO CHANGE)

By *14 Nov 58*  
NAME AND

*AMB*  
GRADE OF OFFICER MAKING CHANGE)

*20 MAR 61*  
DATE

CLASSIFIED DOCUMENT

This material contains information affecting the National Defense of the United States within the meaning of the espionage laws, Title 18, U.S.C., Secs. 793 and 794, the transmission or revelation of which in any manner to an unauthorized person is prohibited by law.

NATIONAL ADVISORY COMMITTEE  
FOR AERONAUTICS

WASHINGTON  
November 16, 1953

RECEIVED SENATOR



0143278

NACA RM E53H25

~~CONFIDENTIAL~~

## NATIONAL ADVISORY COMMITTEE FOR AERONAUTICS

RESEARCH MEMORANDUMJET EFFECTS ON FLOW OVER AFTERBODIES IN  
SUPERSONIC STREAM

By Edgar M. Cortright, Jr., and Fred D. Kochendorfer

## SUMMARY

Current NACA research on the subject of jet effects on the flow over afterbodies in a supersonic stream is briefly summarized. Several jet nozzle types installed in various afterbody configurations are considered for a wide range of operating conditions.

## INTRODUCTION

Increased attention is currently being directed to the problem of afterbody aerodynamics, since afterbody drag frequently represents an appreciable portion of the total body drag of aircraft and missiles. In the case of engine-in-fuselage and nacelle configurations, the problem of predicting the flow field over afterbodies or boattails is complicated by interference effects from the propulsive jet that issues from the base of the body. This jet disturbs a flow that is already contaminated by heavy boundary layer and that is subject to wing and tail interference effects. In addition, the flow is attempting to negotiate the adverse pressure gradient usually present over at least the rearmost portions of the boattail. Consequently, the details of the problem are complex.

In the present report an attempt is made to summarize some of the results of current NACA research on the problem of jet effects. Emphasis is placed on providing a definition of the various phases of the problem, as well as on presenting some of the important concepts and parameters that contribute to the understanding of these phases. Previous research on the subject of jet effects on external aerodynamics may be found in references 1 to 7. The majority of the data contained herein were obtained from recent unpublished sources.

~~CONFIDENTIAL~~~~CONFIDENTIAL~~

3052

T-20

## APPARATUS

Four of the models used to determine jet effects on the flow over afterbodies for the present report are illustrated in figure 1. The earliest model (upper left) utilized a half-sting with splitter-plate arrangement, wherein the unheated jet air was reversed in direction within the body and discharged through half an afterbody. This model is more fully described in reference 5. The two small strut-mounted models (lower), which have provided most of the data presented herein, differ from each other in that one utilizes an oxygen-alcohol rocket engine for a gas supply, while the other (described in ref. 8) utilizes unheated air. Support interference effects appear to be larger where side struts are used. The most recently utilized is the large-scale strut-mounted model for the 8- by 6-foot tunnel (upper right). This model has a gasoline combustor, which makes possible jet temperatures from atmospheric to 2500° F. Forces and pressures on the nozzle and body may be independently measured.

## SYMBOLS

The following symbols are used in this report:

A	cross-sectional area
$C_D$	drag coefficient, $D/q_0 A_B$
$C_{D,b}$	annular base drag coefficient, $D_b/q_0 A_b$
$C_p$	pressure coefficient, $(p - p_0)/q_0$
$C_{p,b}^*$	base pressure coefficient referenced to conditions ahead of base, $(p_b - p_a)/q_a$
D	drag force
d	diameter
M	Mach number
m	mass flow
P	total pressure
p	static pressure
$\left(\frac{\Delta p}{q}\right)$	pressure-rise coefficient

$\left(\frac{\Delta p}{q}\right)$  mean pressure-rise coefficient,  $\frac{1}{2} \left( \frac{p_w - p_b}{q_i} + \frac{p_w - p_b}{q_e} \right)$

$q$  dynamic pressure,  $\gamma \rho M^2 / 2$

$R$  gas constant

$Re$  Reynolds number

$T$  total temperature

$V$  velocity

$x$  axial distance upstream of base

$\beta$  angle of boattail at rearmost station, deg

$\delta$  thickness of boundary layer at point where the velocity equals 0.99 times the local stream velocity

$\epsilon$  angle of nozzle at exit station, deg

$\gamma$  ratio of specific heats

$\nu$  angle that edge of jet stream makes with body axis immediately after leaving nozzle, deg

$\psi$  angle that external stream makes with body axis immediately after separating from end of boattail, deg

#### Subscripts:

$a$  boattail station just upstream of base, no jet flow

$B$  body maximum

$b$  annular base

$e$  local stream conditions along external free streamline after separation from boattail

$i$  local stream conditions along jet free streamline after separation from nozzle

$j$  jet conditions at nozzle exit

$n$  nozzle exit

s base bleed air measured at exit station, or ejector secondary air  
 t throat  
 w wake conditions downstream of interaction point of jet and  
 external streams  
 O free stream

## RESULTS AND DISCUSSION

### Parameters and Nomenclature

Before the results of this research are considered, it is necessary to define some of the geometric and flow parameters inherent in the problem. A typical conical afterbody is depicted in figure 2(a). Both the jet and external flow are from left to right. Important geometric parameters are the boattail angle or contour and the diameters of the body, the base, and the nozzle exit. The pressures of interest include the free-stream pressure  $p_0$ , the boattail pressures  $p$ , the pressure just ahead of the base  $p_a$ , the base pressure  $p_b$ , and the jet static pressure  $p_j$ . In addition, the jet total pressure  $P_j$  and total temperature  $T_j$  are of importance.

A variety of nozzle configurations discharging various types of jet streams through the exit opening in the base may be encountered in practice. Several representative types that have been investigated are shown in figure 2(b). The simplest of these is the convergent nozzle, which is retained in the analysis for reference purposes, even at the higher Mach numbers where convergent-divergent or ejector nozzles would be required to yield maximum thrust potential. The convergent-divergent nozzle has an increasing ratio of exit diameter to throat diameter  $d_n/d_t$  as the design pressure ratio increases. The nozzle-exit angle  $\epsilon$  is not necessarily zero for this nozzle or for the other nozzles. With the ejector nozzle, the ratio of exit diameter to throat diameter also increases as the design pressure ratio increases. In addition, however, a supply of secondary air is provided to cushion the expansion of the primary stream and thus provide more nearly isentropic flow. When blunt annular bases are present and exhibit negative pressures, air is sometimes discharged into the base region in order to realize the drag-reducing effects of base bleed; this case is also briefly treated.

## Jet Effects on Boattail Pressures

3052

Jet effects on boattail pressures are shown qualitatively in figure 3(a) for the case of supersonic flight. The physical phenomena are illustrated in the upper portion of the figure, which depicts the effects of the jet from a convergent nozzle on the flow over a  $5.6^\circ$  conical boattail. The jet, which is shown at a higher than ambient static pressure at the exit, expands on leaving the nozzle and thus deflects the external stream. If the flow were inviscid, a shock wave would originate precisely at the meeting point of the internal and external streams, and a pressure discontinuity would exist. The presence of the body boundary layer with its low-energy subsonic region precludes the possibility of a discontinuous rise in pressure, with the result that the required pressure rise begins ahead of the shock wave, where the boundary layer thickens and originates compression waves. If the deflection is sufficiently great and the shock wave sufficiently strong for the particular state of the boundary layer, the flow will be separated from the boattail, inasmuch as the low-energy regions of the boundary layer are unable to negotiate the required pressure rise. Translation of these simple concepts into quantitative form is most difficult, with the result that there is no current method to predict the magnitude of jet effects on boattail pressures. It may be possible, however, to approximate the onset of separation by use of the critical-pressure-rise-coefficient concept (ref. 8). Experimental boattail pressure distributions are plotted in figure 3(a) for various values of the jet static-pressure ratio  $p_j/p_0$ . For values of  $p_j/p_0$  appreciably in excess of one, considerable thrust existed over the rearmost portions of the boattail.

## Modifying Factors

Many factors influence the exact nature of jet effects on boattail pressures. Some of these factors are illustrated in figure 3(b). The jet interference decreases with decreasing overpressure at the exit, which may result from either reduced jet total pressure or from increased expansion within the nozzle. Also, the presence of an annular base can partially or entirely shield the boattail from jet interference, depending on the size of the annulus, because the internal and external streams separate from the body and meet downstream of the base. The jet then influences the base pressure but will usually not influence the boattail pressure until the base pressure had risen sufficiently far above the rearmost pressure on the boattail. The jet effect is increased by the use of a large boattail angle, which increases the strength of the trailing shock wave, increases the adverse pressure gradient over the boattail, and thus makes it more susceptible to flow separation. Lastly, the use of large nozzle-exit angles may result in a relative increase in the trailing-shock strength and hence in an increased jet effect.

~~CONFIDENTIAL~~

With angle of attack or yaw at supersonic speeds, the jet interference has been found to be asymmetrical, which causes a destabilizing shift in the body center of pressure, and which may influence nearby control surfaces. Angle-of-attack effects are beyond the scope of this paper, however.

### Jet Effects on Boattail Drag

Some jet effects on boattail pressure drags at a free-stream Mach number near 2.0 are presented in figure 4 in order to illustrate the qualitative considerations discussed in the previous section. The variation with boattail shape of the drag-reducing effect of a jet from a convergent nozzle is shown. In the case of the three conical boattails of base-to-body diameter ratio of 0.5, the drag with no jet increased considerably as the boattail angle increased. The jet interference also increased, however, so that all three boattails experienced a pressure-drag reduction approaching 25 percent at a jet total-pressure ratio of 14. The highly sloping parabolic afterbody ( $\beta = 17.2^\circ$  at rearmost station) experienced a much greater jet interference; so that, at the higher pressure ratios, the drag was reduced over 40 percent to a value less than the drag of a conical boattail of equivalent length (i.e.,  $\beta = 8.8^\circ$ ). Drag data were obtained by integration of pressure distributions on small-scale models in the case of the conical boattails (ref. 5); the parabolic boattail drags were obtained in the same manner from experiments in the 8- by 6-foot tunnel where they were checked by force measurements.

It may be noted that the larger drag reductions in the case of the parabolic afterbody were obtained despite the presence of a slightly larger annulus than was present on the sharp-edge conical boattails, although annular pressure forces are not included in these drag data. Actually, a small annulus corresponding to this base-to-nozzle diameter ratio of 1.11 appears to afford little shielding of the boattail, even in the case of the low-angle boattails. However, with a larger annulus ( $d_p/d_n = 1.41$ ), the boattail drag for the three conical boattails was virtually invariant with jet pressure ratio.

Figure 4 also illustrates that, as nozzle-exit angle  $\epsilon$  increased, the favorable jet interference effects for both the convergent and the convergent-divergent nozzles also increased. Increasing the nozzle-exit angle  $12^\circ$  in the case of the convergent nozzle resulted in the indicated downward displacement of the drag curve. In the case of the convergent-divergent nozzle,  $\epsilon$  was increased  $18^\circ$  with the same effect. It may be noted that no large drag reductions resulted from the convergent-divergent nozzles until the nozzle design total-pressure ratio was appreciably exceeded, thus creating an overpressure condition

The amount of drag reduction which may occur below design pressure ratio is dependent on the nozzle and boattail details.

### Pressure-Rise Coefficient

Before the pressures that act on annular blunt bases are discussed, it is instructive to consider the concept of critical-pressure rise with the aid of figure 5. A foreward-facing step would theoretically create a detached bow wave in supersonic inviscid flow; however, the presence of a boundary layer results in a separated flow pattern of the type indicated in the figure. In reference 9 it was originally proposed that a critical-pressure-rise coefficient be defined as the change in static pressure from a station upstream of the separation point to a station in the separated flow region divided by the upstream dynamic pressure. Furthermore, it was suggested that the coefficient  $\left(\frac{\Delta p}{q}\right)$  is proportional to  $Re^{-1/5}$  for turbulent boundary layers for any given Mach number and that it might be applied to correlate other flow phenomena of a somewhat related nature. Additional experimental evidence (ref. 10) indicates that the effect of Reynolds number for turbulent boundary layers is negligible. It is also shown in reference 10 that the experimentally determined pressure-rise coefficient for a blunt step is in approximate agreement with that of a two-dimensional airfoil (defined as indicated) and that this pressure-rise coefficient varies with Mach number. If the blunt step is rearward-facing, experimental data from reference 11 indicate  $\left(\frac{\Delta p}{q}\right)$  to be invariant with Mach number at a value of approximately 0.36.

If a section of a blunt annulus is considered, it is immediately apparent that the flow is similar to but more complex than the aforementioned cases. In this case the two streams that separate from the surface of the nozzle and body are generally inclined at different angles and are at different levels of pressure, temperature, and Mach number. In addition, the state of the boundary layers is markedly different in the two streams. However, it is possible to define a mean pressure-rise coefficient  $\overline{\left(\frac{\Delta p}{q}\right)}$ , which is the average of pressure-rise coefficients based on the internal and external streams. Unfortunately, the reduction of experimental base, body, and nozzle pressures to yield a value of  $\left(\frac{\Delta p}{q}\right)$  requires a knowledge of the external and internal stream curvatures after separation, since a two-dimensional solution of this flow field is markedly inadequate. Most of the values of  $\overline{\left(\frac{\Delta p}{q}\right)}$  presented herein were obtained by using schlieren photographs to determine jet curvature and by using a few existent characteristic solutions for the curvature of the separated



external flow. As a result, these values must be considered as only a crude first effort, pending more accurate theoretical treatment; such treatment will require the determination by characteristics of a great many overpressure jet shapes and, although they are less significant, the free streamlines of some separated external flows.

The important fact to observe in figure 5 is not that behavior of the individual variations, which may indicate scatter, was somewhat irregular, but rather that most of the values of mean pressure-rise coefficient for the convergent nozzles at both Mach numbers fell between 0.3 and 0.4, the range to be expected from the experiments with steps and airfoils. Although the data are presented only for conical boattails of  $5.6^\circ$ , boattails with values of  $\beta$  from  $0^\circ$  to  $11^\circ$  also yielded values of  $\left(\frac{\Delta p}{q}\right)$  in this range. In the case of the convergent-divergent nozzles designed for a pressure ratio of 10.5, only data obtained with a small annulus are presented, since sufficient information to correct the data for three-dimensional effects was not available. A two-dimensional solution, which may not be much in error for a small annulus, was thus utilized. Again the mean pressure-rise coefficient varied only slightly over a wide range of pressure ratios, but the values were below those obtained with a convergent nozzle; a satisfactory explanation for the discrepancy in values is not known at this time. Attempted correlation of  $\left(\frac{\Delta p}{q}\right)$ ,  $\frac{\Delta p}{q_e}$ , and  $\frac{\Delta p}{q_1}$  with the basic variation of pressure-rise coefficient with Mach number for a step (ref. 10) was inconclusive. In general, it can be concluded that the concept of mean pressure-rise coefficient is a unifying one, but one that requires additional study.

#### Jet Effects on Base Pressure

In figure 6(a) the actual behavior of annular base pressure is shown for a variety of nozzle and boattail geometries and for a wide range of operating pressure. Base pressure coefficient is plotted as a function of jet static-pressure ratio for  $5.6^\circ$  conical boattails at a Mach number of 1.9. Initial base pressure coefficients for no jet flow are indicated on the ordinate. The clarity of this figure is enhanced if the jet effect for a typical geometry is first studied.

For a convergent nozzle with  $d_b/d_n$  of 1.11, a slight amount of jet flow produced an appreciable increase in base pressure; further increases in jet pressure, and thus in jet flow, resulted in the jet stream aspirating the annulus to a lower pressure. However, as the jet pressure increased still further, the jet expanded more and increased the strength of the trailing shock wave at its juncture with the external stream. The

wake pressure thus increased; and the existence of a mean pressure-rise coefficient forced the base pressure to increase also. As the base diameter becomes larger relative to nozzle-exit diameter, the expanding jet flow curves increasingly toward the axis before meeting the external flow, which would decrease the angle of interaction between the two streams if the base pressure remained constant. Thus, in order to main-

tain a nearly constant value of  $\left(\frac{\Delta p}{q}\right)$ , a larger initial expansion angle corresponding to a lower base pressure coefficient must exist for the given jet pressure ratio, as is seen to be the case. The portions of these curves corresponding to jet total pressures below those producing minimum base pressures are not included, except in the single illustrative case.

Compressed into the lower end of the pressure-ratio range are the variations of base pressure coefficient with a convergent-divergent nozzle having an expansion ratio corresponding to a design total-pressure ratio of 10.5. A nozzle of this type has a design static-pressure ratio of 1 and requires a total-pressure ratio of 21 to operate at a static-pressure ratio of 2. The variations are essentially parallel to the corresponding variations with convergent nozzles but are displaced slightly in the positive direction. Included is a single variation obtained with an ejector nozzle designed for the same pressure ratio; the base pressures obtained were somewhat higher than might be expected from the other data. It is believed that there is a logical reason for this, however. The secondary weight flow, which was 4 percent of the primary weight flow  $\left(m_s/m_j\right) \sqrt{T_s/T_j} = 0.04$ , created a layer of relatively low-energy air around the primary jet stream that might be expected to lower the limiting pressure rise across the trailing shock and thus increase the base pressure.

A practical comparison of the effects of jets from a convergent and a convergent-divergent nozzle is illustrated by the case of a jet total-pressure ratio of 10.5 corresponding to a turbojet engine at a Mach number of 1.9. The convergent nozzle, with its static-pressure ratio near 5, generally increased the base pressure over its no-flow value, except for extremely large annuli, and generated appreciably positive base pressures in some cases. The convergent-divergent nozzle ( $\epsilon = 0$ ), however, with its jet static-pressure ratio of 1, decreased the base pressures below the no-flow values with the resulting tendency to create relatively large base drags. An additional point of interest on this figure is the fact that replacing the idealized blunt base with a  $45^\circ$  bevel, such as might occur with an iris or clamshell nozzle, did not greatly alter the basic variation of base pressure with jet pressure for the case of  $d_b/d_n$  of 1.67. This result was also found with a convergent-divergent nozzle.

This entire family of pressure variations for the convergent nozzle could be crudely reproduced theoretically, with only a value of

$\left(\frac{\Delta p}{q}\right) = 0.35$  given, except possibly the  $d_b/d_n = 1.11$  variation. An indication of the approximate order of accuracy is given by the fact that, for the case of  $d_b/d_n = 1.4$  and  $p_j/p_0 = 4$ , a variation of 0.04 in  $\left(\frac{\Delta p}{q}\right)$  results in a variation of 0.04 in base pressure coefficient. However, it should be remembered that a more accurate analysis of this approach is required.

3052

### Effect of Stream Mach Number

The effect of stream Mach number on these characteristic curves is shown in figure 7, in which data obtained at Mach numbers of 0.9 and 3.1 are given, and data at a Mach number of 1.9 are reproduced in part for reference. The same boattails and nozzles were used throughout.

In order to obtain the data at a Mach number of 0.9, the afterbodies were mounted on the end of a pipe that extended through the tunnel bell-mouth into the cylindrical test section. With no jet flow, the base pressure was found to vary considerably with boattail shape. As the extent of boattailing increased, corresponding to smaller bases and lower values of  $d_b/d_n$ , the external stream was diffused more before separation at the base; hence the base pressure increased. Boattail angle also had an appreciable effect, but treatment of this parameter at subsonic speeds is beyond the scope of this paper. The action of the jet bears a certain similarity to that observed at supersonic speeds. With a small annulus, the expanding jet tends to impede the flow near the annulus, with a resultant increase in pressure. Since subsonic flow will tolerate no abrupt changes, these increases in base pressure are also indicative of increases in pressures on the boattail. For large base annuli, the jet turns axially before meeting the external flow in this pressure-ratio range and, rather than decelerating the flow, pumps the base and boattail pressures to lower values. Higher jet pressure ratios, however, seem to reverse the direction of the curves as at supersonic speeds. Comparison of the curves with those obtained at a Mach number of 1.9 in the same pressure-ratio range shows the general resemblance at the two Mach numbers as well as the larger spread in base pressure coefficients existing at the high subsonic speeds. The data at Mach number of 0.9 have not been corrected for wind-tunnel wall interference; such a correction would be expected to decrease the values of base pressure coefficient.

At a Mach number of 3.1, the effect of increased Mach number in reducing the total spread of this family of curves is again seen; the jet effect on base pressure coefficient is appreciably reduced. The correlation of the effect of convergent and convergent-divergent nozzles is even more striking at this Mach number, where, for the same jet static-pressure ratio, the base pressure is nearly the same with either nozzle

type (again neglected is the pressure-ratio range below those values producing the minimum base pressures). In addition, for the case of a diameter ratio  $d_b/d_n$  of 1.4, convergent-divergent nozzles designed for pressure ratios from 10.5 to 50 yielded essentially the same base pressure variation. The no-flow values of base pressure are also indicated on the ordinate but are unlabeled, since they follow the same order as the curves with flow. With the range of annulus sizes likely to be encountered ( $d_b/d_n \leq 1.4$ ), the convergent nozzle usually produces base thrusts at values of jet static-pressure ratio corresponding to the various flight Mach numbers. With the same annulus sizes, the convergent-divergent nozzles generally produce base drag at supersonic speeds.

### Effect of Boattail Geometry

The base pressure coefficients presented so far were obtained with a specific family of afterbodies. Changes in afterbody geometry do not alter the basic trends, provided the flow remains unseparated over the boattail, but they do change somewhat the pressure level of the family of characteristic curves. For two convergent nozzles, the effect of changing conical boattail angles is shown in figure 8. The data were obtained with a jet total-pressure ratio of 8, but the analysis applies to other pressure ratios as well. Two forms of base pressure coefficient, the conventional  $C_{p,b}$  and also  $C'_{p,b}$ , are utilized. The coefficient  $C'_{p,b}$ , originally used in reference 12 for bodies of revolution, essentially references the base pressure to conditions just ahead of the base and is thus a measure of the change in pressure from the end of the boattail to the base. Adding  $C'_{p,b}$  to the pressure coefficient just upstream of the base yields  $C_{p,b}$  approximately.

As the boattail angle increases, the expansive turning at the base decreases and can turn to compression; the value of  $C'_{p,b}$  thus increases in the positive direction. However, with a fixed base diameter, the pressure ahead of the base generally decreases and results in only a moderate variation in the conventional base pressure coefficient with boattail angle. The curves are predicted variations obtained from the data for  $\beta = 5.6^\circ$  and from assumptions similar to those of reference 5, which have had limited success in estimating the effects of boattail shape on base pressure with no jet at supersonic speeds. The flow-separation angle  $\psi$ , calculated from the initial data, is assumed to remain invariant with boattail shape for the particular jet pressure ratio and value of  $d_b/d_n$ . Combining the resulting values of  $C'_{p,b}$  with values of  $C_{p,a}$  predicted for inviscid flow by reference 13 yielded the indicated variation of  $C_{p,b}$ . Agreement with experiment is not always this good, and the method breaks down if the flow separates ahead of the base. To further illustrate this assumption, if the conical

boattail angle is held constant and the nozzle scaled up to yield a shorter boattail while maintaining the fixed value of  $d_b/d_n$ , the following result would be predicted: The pressure ahead of the base would decrease without a change in the value of  $C'_{p,b}$  and would thus lower the base pressure coefficient  $C_{p,b}$  below the value obtained with the longer boattail. The apparent success of this simple estimate in some cases may be fortuitous, since a fixed value of  $\psi$  may not be at great variance with a fixed value of mean pressure-rise coefficient. The following table presents values of  $C_{p,a}$  for the afterbodies considered herein, so that  $C_{p,b}$  may be converted to  $C'_{p,b}$  for use with other afterbody shapes:

Free-stream Mach number, $M_0$ , 1.9					
$\beta$	$d_b/d_n$				
	2.67	2.0	1.67	1.4	1.11
3		0			
5.6	0.018	-.035	-0.01	0	0.03
7				-.005	
11				-.049	
Free-stream Mach number, $M_0$ , 3.1					
5.6	-0.016	-0.04		-0.027	1.022

#### Effect of Nozzle-Exit Angle

It was shown in the case of jet effects on boattail pressure that increasing the nozzle-exit angle increases the strength of the trailing shock and hence the interference effect. From a consideration of

$\left(\frac{\Delta p}{q}\right)$ , the same result is expected with an annular base. In figure 9

the effect of nozzle-exit angle on base pressure is shown for the case of three nozzle angles in two afterbodies at  $M_0 = 1.6$ . Pertinent geometric parameters are indicated. The data, which were obtained by C. A. de Moraes at the NACA Langley laboratory with solid propellant rocket gases, clearly indicate that increased nozzle-exit angles increase the annular base pressure.

#### Effect of Jet Temperature

The consideration of rocket gases gives rise to the problem of the applicability of data obtained with unheated jet fluids, which is considered in figure 10. Data were obtained for a fixed model geometry with

3053

unheated air, unheated carbon dioxide, and the products of combustion of an oxygen-alcohol rocket used for jet fluids. The use of carbon dioxide with a ratio of specific heats  $\gamma$  of 1.3 produced a moderate upward shift in the curve. The rocket gases produced a much larger increase in the base pressures. Data are also presented that were obtained with the large-scale model in the 8- by 6-foot tunnel with unheated and heated air. The effect of heating the air to 2500° R was to raise the curve slightly. Thus, the use of data obtained with unheated air is conservative, in that the values of base pressure are too low.

Analysis of the temperature effect is complicated by variations in  $\gamma$ ,  $T$ , and  $R$ , which affect the jet shape and mixing and hence the expected value of mean pressure-rise coefficient  $\left(\frac{\Delta p}{q}\right)$  across the trailing shock.

However, the results are presented for a simple empirically derived calculation to estimate the temperature effects by consideration of the  $\gamma$  of the jet. The assumption was made that the jet total pressures that produce the same base pressure for various values of  $\gamma$  and any given nozzle-afterbody combination are those which yield the same value of jet exit angle  $\nu$ . With this assumption it was possible to correct the data at  $\gamma = 1.4$  to other values of  $\gamma$  as indicated by the dashed lines. This correction appears adequate for correlating the air and carbon dioxide data from the small-scale experiments as well as the hot- and cold-air data from the 8- by 6-foot tunnel. In addition, the correction correlates boattail pressure drags for the large model. The good agreement is perhaps fortuitous, since the data obtained with a rocket are not predicted with even the lowest possible value of  $\gamma$ . Several considerations, such as the unknown temperature and velocity distributions at the nozzle exit, the possibility of burning downstream of the nozzle exit, and the appearance of a layer of water flowing over portions of the internal nozzle surface, make conclusions difficult, however. Additional research is obviously required.

#### Effect of Reynolds Number

Another question that arises in considering the validity of small-scale unheated-jet effects is the influence of Reynolds number, which was investigated briefly as indicated in figure 11. The effective Reynolds number of a turbulent boundary layer was varied in three ways and the influence on jet effects determined. In the first case, Reynolds number  $Re$  was varied by running similar models in the 18- by 18-inch ( $M_0 = 1.9$ ) and the 8- by 6-foot ( $M_0 = 2.0$ ) tunnels at values of  $Re$  of  $5.5 \times 10^6$  and  $35 \times 10^6$ , respectively. The jet effects on base pressure were nearly identical. Also at a Mach number of 1.9 and a low Reynolds number, the thickness of the boundary layer ahead of the base was increased  $3\frac{1}{2}$  times by artificial transition (ref. 5), with only a



small increase in base pressure. Lastly, at a Mach number of 3.1, the Reynolds number was appreciably increased by a change in tunnel pressure, with only a slight decrease in base pressure. It might thus be concluded that, as in the case of plain bodies of revolution, Reynolds number has only a small effect on base pressure, provided the boundary layer is turbulent ahead of the base. This result is consistent with the fact that critical-pressure-rise coefficient is relatively independent of Reynolds number for turbulent boundary layers.

#### Annular Base Bleed

In figure 12 the case is considered in which a blunt annulus is present and where it is desired to reduce the base drag by discharging air from the annulus, as proposed in reference 14 (see also ref. 15). Since blunt bases with convergent-divergent nozzles exhibit the most drag, it would be desirable to study such a case; however, because of model limitations, it was necessary to simulate this case with a convergent nozzle at low pressure ratio. For the case illustrated,  $d_b/d_n = 1.4$ . The base drag coefficient (based on annular base area) with bleed flow may be expressed as the sum of three terms: (1) that due to base pressure, (2) that due to exit velocity, and (3) that due to inlet momentum (indicated as free-stream momentum). The sum of terms (1) and (2) represents the exit total momentum. This quantity drops rapidly from a positive to a negative drag (thrust) as the bleed total pressure increases. Also, as shown in the right-hand portion of the figure, the bleed weight flow increases. If the bleed air is charged with the full free-stream momentum ((1) + (2) + (3)), there is only a small initial reduction in drag and then an increase that levels out with large weight flows. Thus, as in the case of plain bodies of revolution, if air is to be taken aboard for the express purpose of reducing base drag, it should not come from a free-stream inlet but rather from a low-energy source. For example, with an unheated jet the data indicate that a bleed flow of 1.7 percent of the jet flow could be obtained by venting the annulus to ambient static pressure. If the induced flow came primarily from the low-energy region of the boundary layer with negligible momentum charge, the base drag would be eliminated. In cases in which the air must be taken aboard for air-conditioning or tail-pipe cooling, the inlet momentum charge to the aircraft cannot be avoided and it appears that a blunt annulus, if present, is a good place to discharge the air.

Base-burning schemes, such as suggested in references 16 and 17, may be quite effective in reducing base drag, but are more difficult to apply to aircraft.

### Total Afterbody Drag

Many of the important parameters influencing jet effects on base pressure have now been considered. Figure 13 is presented to illustrate both the utility of the data and the fact that annular base pressure may influence the choice of afterbody designs. Afterbody drag coefficient, including jet interference effects, is presented as a function of base-to-nozzle-exit diameter ratio for both convergent and convergent-divergent nozzles with the same throat areas and with axial exit flow. The curves are predicted with the aid of the data of this report and the results of references 5 and 12. Only the case of a small boattail angle is considered at a Mach number of 1.9 with a jet total-pressure ratio of 10. In the case of the convergent nozzle, the total afterbody drag initially decreases slightly as the base diameter is increased, because of positive pressures (thrust) on the annulus. Furthermore, a relatively large base annulus may be utilized without incurring any drag penalty at this Mach number. In the case of the convergent-divergent nozzle designed for a pressure ratio of 10, however, the drag is indicated to increase immediately as an annulus is added. It is thus desirable to keep the size of the base annulus to a minimum in order to avoid costly drag penalties.

### CONCLUDING REMARKS

Sufficient investigations of the problem of jet effects on boattail and base pressures have been conducted to clarify many of the important parameters. However, while answering some questions, these studies have served to point out additional problems that should be investigated. With the existing data and some of the concepts presented herein, it appears possible to estimate with limited accuracy the drags of many afterbody nozzle combinations. Thus, although the results may not provide precise drag calculations, they can serve as a guide to good afterbody design practice.

Lewis Flight Propulsion Laboratory  
National Advisory Committee for Aeronautics  
Cleveland, Ohio, August 28, 1953

### REFERENCES

1. Erdmann: Widerstandsbeiwerte für das A4VLP mit Berücksichtigung des Strahl - und Reibungseinflusses für Unter- und Überschallgeschwindigkeiten - Untersuchung der Strahlexpansion. Peenemünde Heeresversuchsstelle Aerodynamisches Institut, Archiv Nr. 66/105, Mars 24, 1943.

~~CONFIDENTIAL~~



2. Purser, Paul E., Thibodaux, Joseph G., and Jackson, H. Herbert: Note on Some Observed Effects of Rocket-Motor Operation on the Base Pressures of Bodies in Free Flight. NACA RM L50I18, 1950.
3. Stoney, William E., Jr., and Katz, Ellis: Pressure Measurements on a Sharply Converging Fuselage Afterbody with Jet on and off at Mach Numbers from 0.8 to 1.6. NACA RM L50F06, 1950.
4. Love, Eugene S.: Aerodynamic Investigation of a Parabolic Body of Revolution at Mach Number of 1.92 and Some Effects of an Annular Jet Exhausting from the Base. NACA RM L9K09, 1950.
5. Cortright, Edgar M., Jr., and Schroeder, Albert H.: Investigation at Mach Number 1.91 of Side and Base Pressure Distributions over Conical Boattails without and with Jet Flow Issuing from Base. NACA RM E51F26, 1951.
6. Gillespie, Warren, Jr.: Jet Effects on Pressures and Drags of Bodies. NACA RM L51J29, 1951.
7. Cantrell, H. N., and Gazley, Carl, Jr.: Base Pressure on Bodies of Revolution at Subsonic and Supersonic Velocities with and without Jet Exhausts. Aero. Fundamentals Memo. No. 18, General Electric Co., Apr. 11, 1952.
8. Rouso, Morris D., and Baughman, L. Eugene: Investigation at Mach Number 1.91 of Spreading Characteristics of Jet Expanding From Choked Nozzles. NACA RM E51L19, 1952.
9. Donaldson, Coleman duP., and Lange, Roy H.: Study of the Pressure Rise Across Shock Waves Required to Separate Laminar and Turbulent Boundary Layers. NACA TN 2770, 1952. (Supersedes NACA RM L52C21.)
10. Love, Eugene S.: The Base Pressure at Supersonic Speeds on Two-Dimensional Airfoils and Bodies of Revolution (with and without Fins) Having Turbulent Boundary Layers. NACA RM L53C02, 1953.
11. Beastall, D., and Eggink, H.: Some Experiments on Breakway in Supersonic Flow, Pt. II. Tech. Note AERO. 2061, British R.A.E., June 1950.
12. Chapman, Dean R.: An Analysis of Base Pressure at Supersonic Velocities and Comparison with Experiment. NACA Rep. 1051, 1951. (Supersedes NACA TN 2137.)
13. Jack, John R.: Theoretical Pressure Distributions and Wave Drags for Conical Boattails. NACA TN 2972, 1953.

14. Cortright, Edgar M., Jr., and Schroeder, Albert H.: Preliminary Investigation of Effectiveness of Base Bleed in Reducing Drag of Blunt-Base Bodies in Supersonic Stream. NACA RM E51A26, 1951.
15. Hebrank, W. H., Scanland, T. S., Platou, A. S., and Hicks, B. L.: The Effects on Base Pressure of Air Ejection from the Base of a Model Projectile at  $Ma = 1.7$  -- Partial Evaluation of the External Ram Jet Principles. Memo. Rep. No. 539, Ballistic Res. Labs., Aberdeen Proving Ground (MD.), Aug. 1951. (Proj. No. TB3-0110V, Res. and Dev. Div., Ord. Corps.)
16. Scanland, T. S., and Hebrank, W. H.: Drag Reduction Through Addition to the Wake of Supersonic Missiles. Memo. Rep. No. 596, Ballistic Res. Labs., Aberdeen Proving Ground (MD.), June 1952. (Proj. No. TB3-0110, Res. and Dev. Div., Ord. Corps.)
17. Baker, W. T., Davis, T., and Matthews, S. E.: Reduction of Drag of a Projectile in a Supersonic Stream by the Combustion of Hydrogen in the Turbulent Wake. CM 673, Appl. Phys. Lab., The Johns Hopkins Univ., June 5, 1951. (Contract NOrd 7386, with Bur. Ord., U. S. Navy.)

~~CONFIDENTIAL~~

NACA RM E53H25

3052

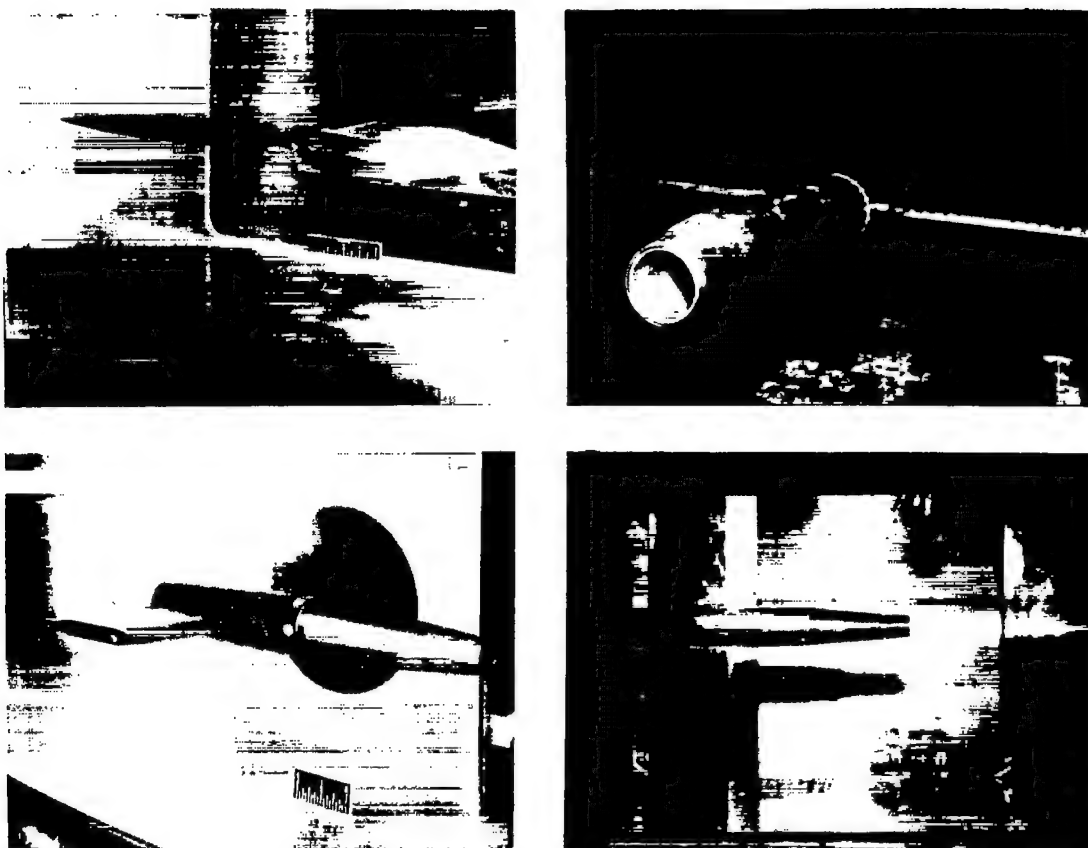
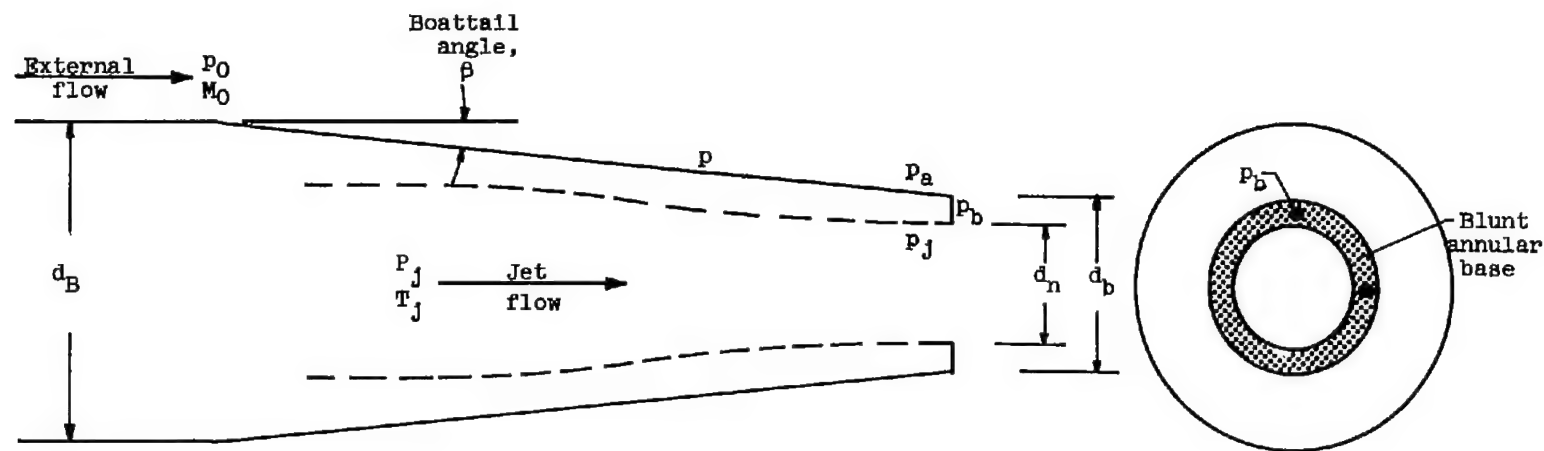


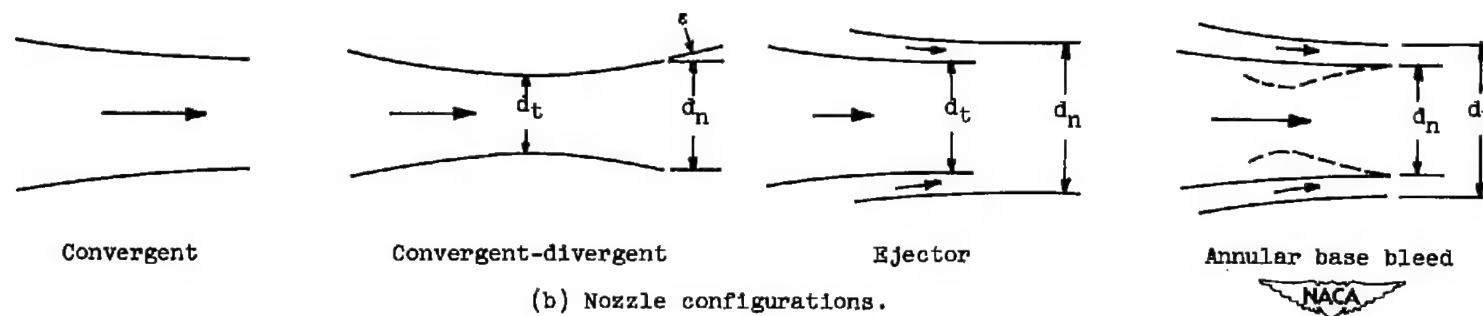
Figure 1. - Jet research models.

NACA  
C-25617  
C-32733  
C-32649  
C-33070

~~CONFIDENTIAL~~



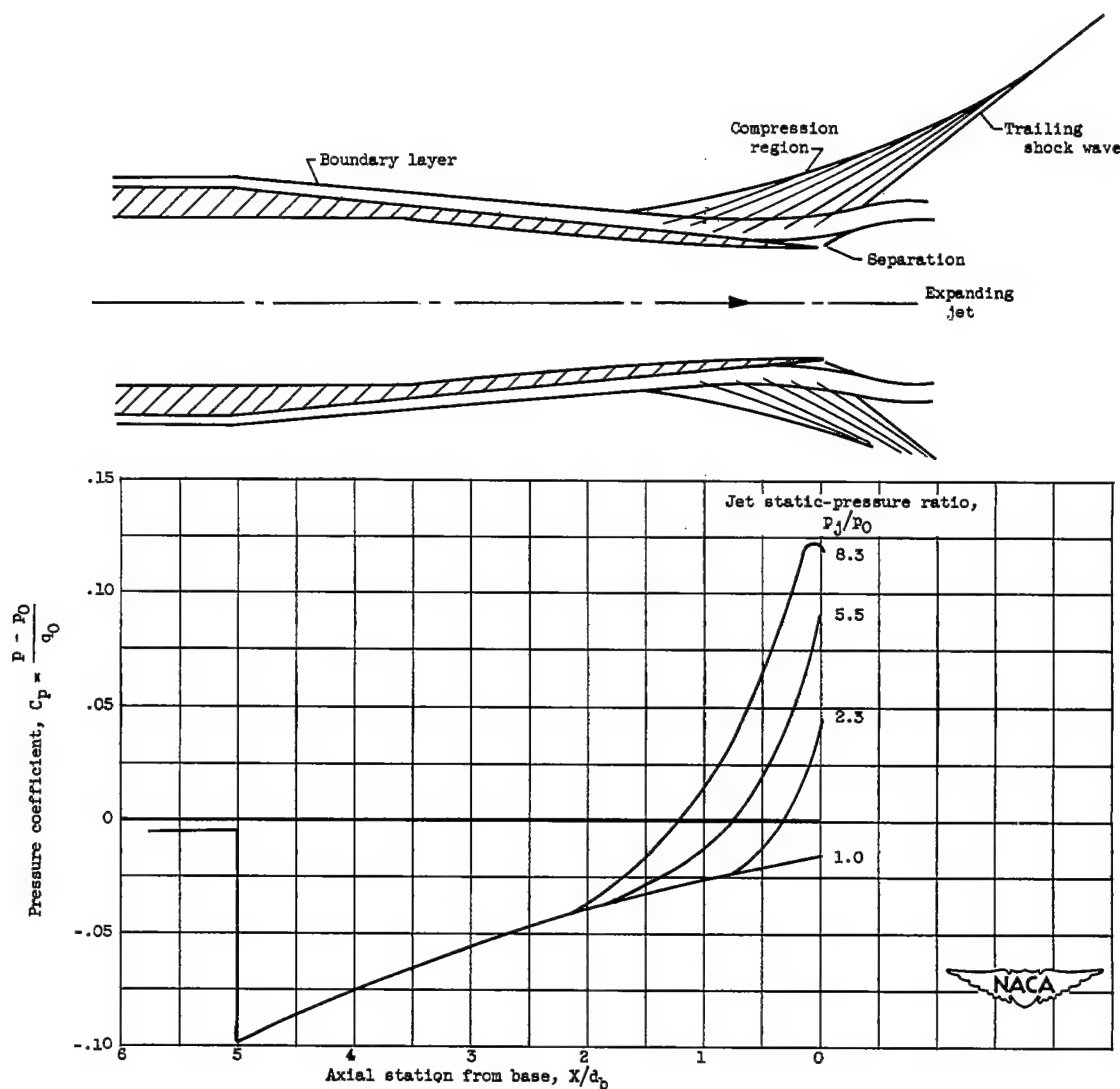
(a) Typical afterbody.



(b) Nozzle configurations.

Figure 2. - Sketch of typical afterbody and several nozzle configurations.

~~CONFIDENTIAL~~

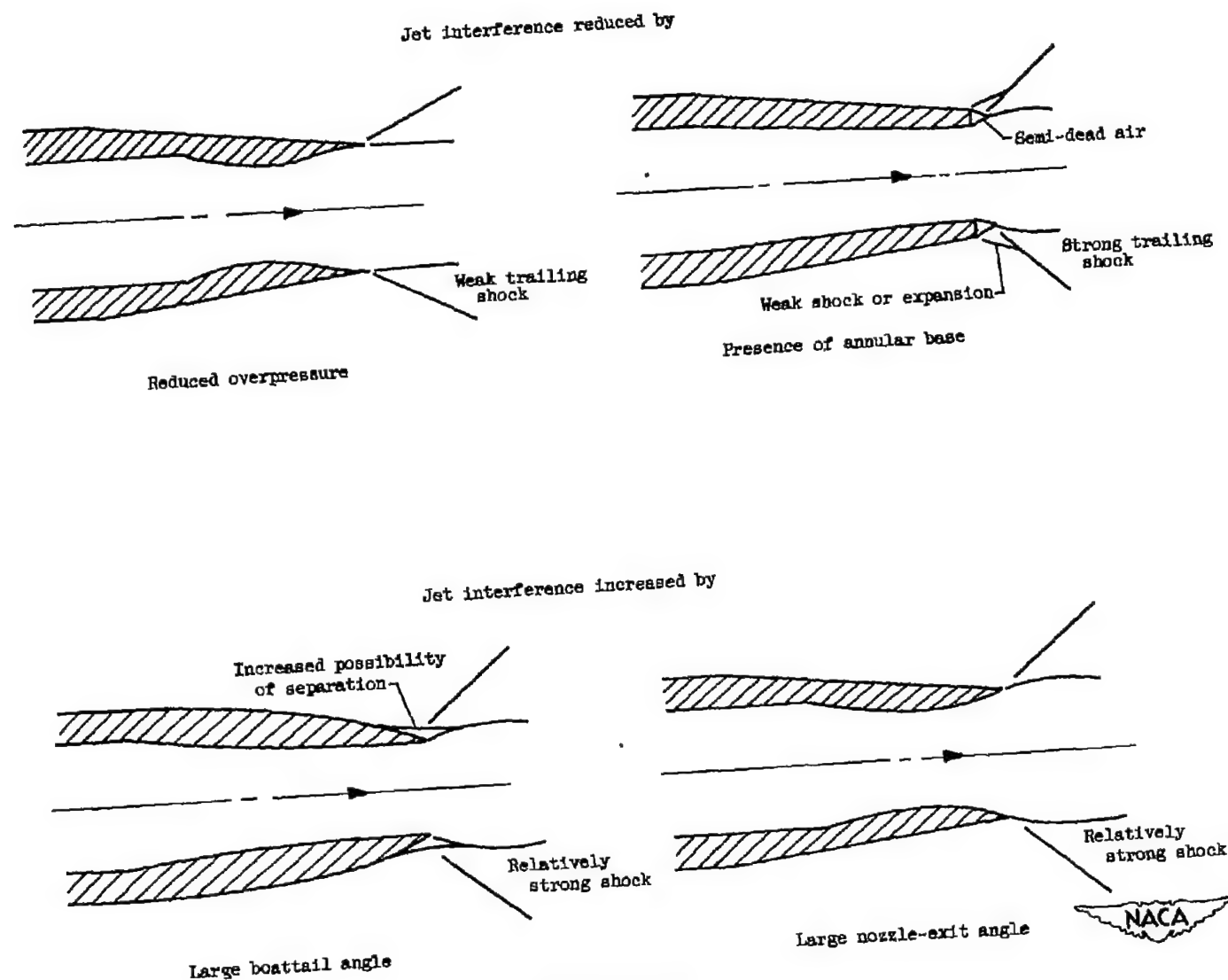


(a) Typical case; free-stream Mach number, 1.9; boattail angle,  $5.6^\circ$ .

Figure 3. - Jet effects on boattail pressures.

~~CONFIDENTIAL~~

3052



(b) Modifying factors.

Figure 3. - Concluded. Jet effects on boattail pressures.

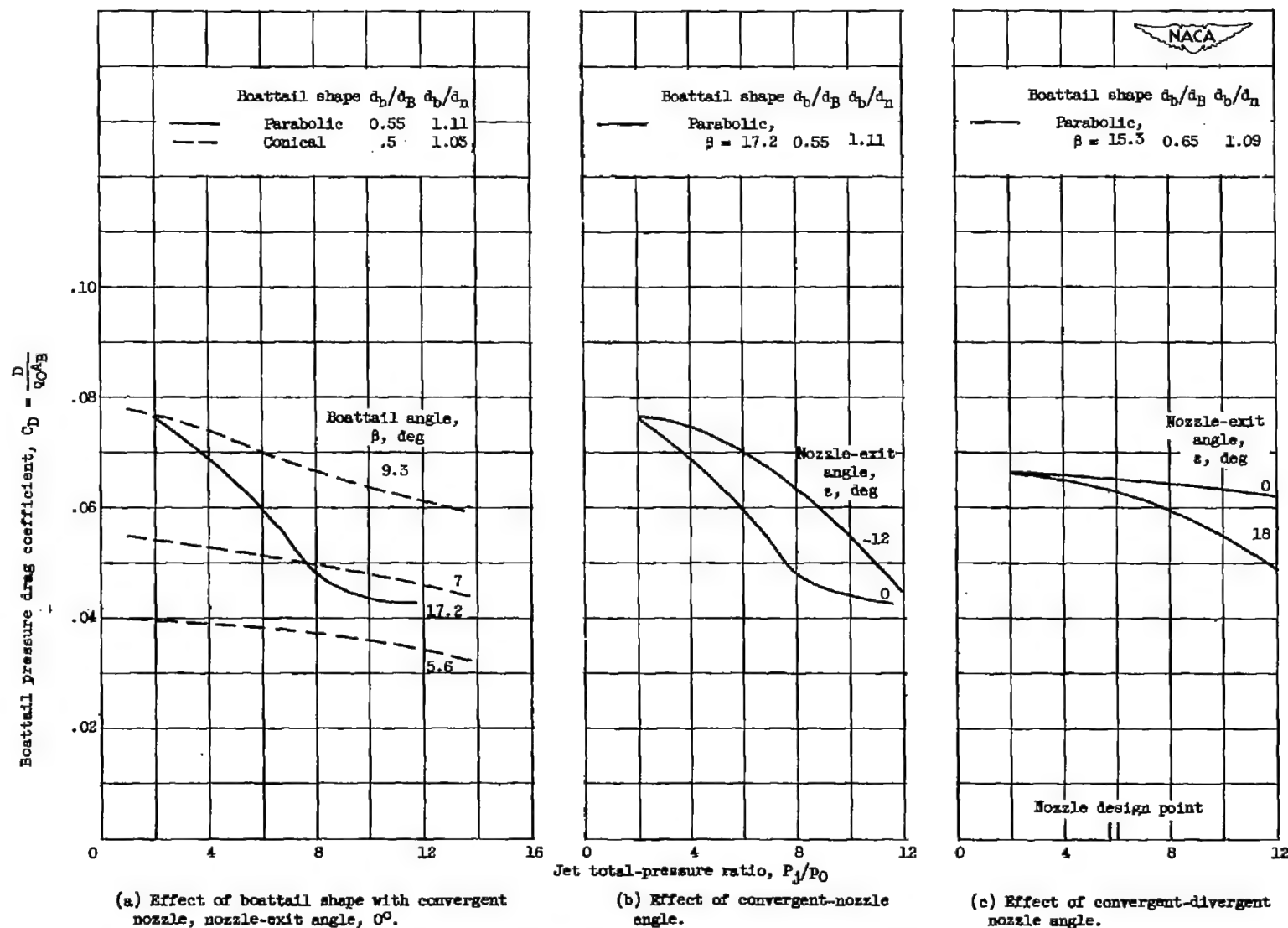


Figure 4. - Jet effects on boattail pressure drag at free-stream Mach numbers of 1.9 to 2.0.

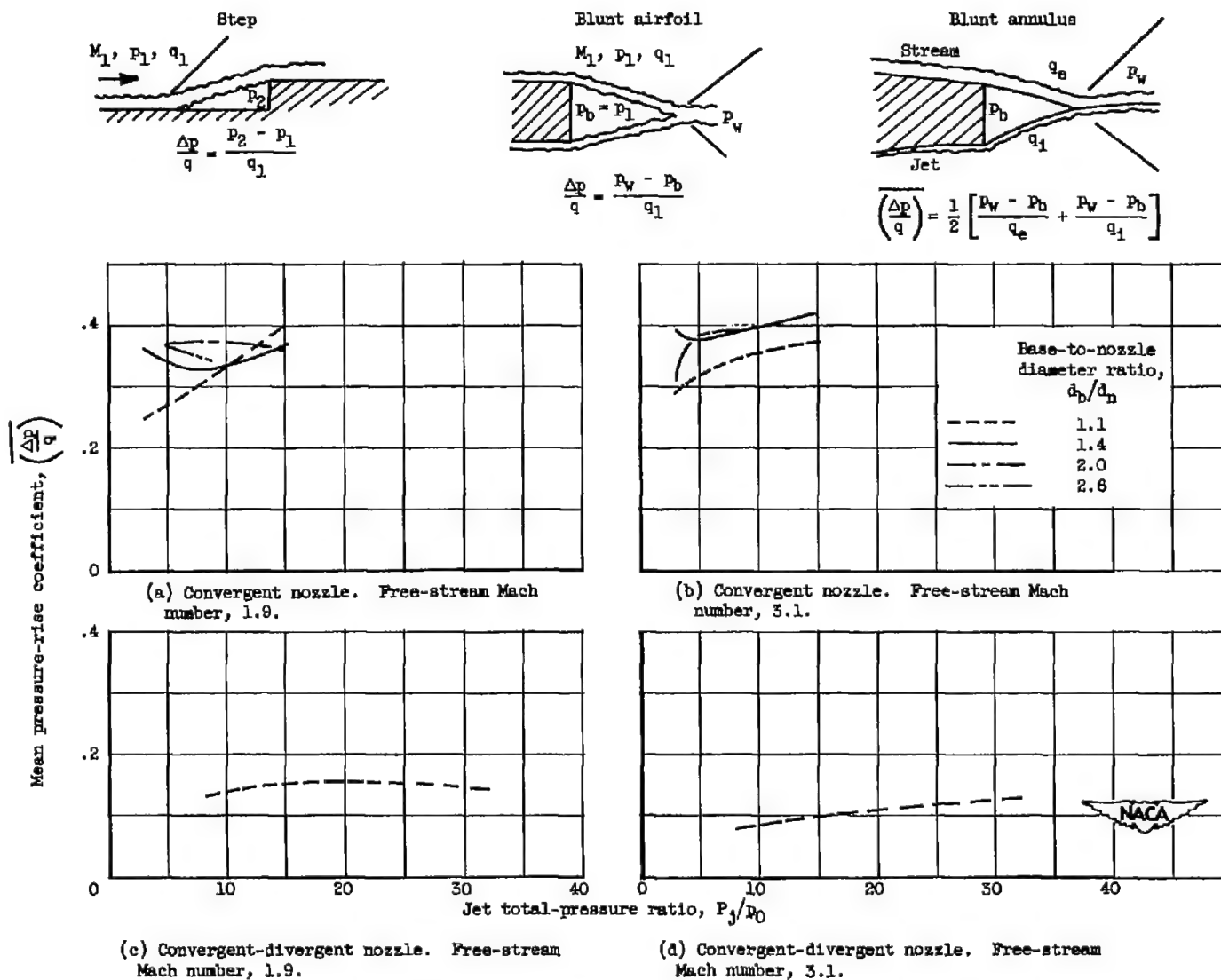


Figure 5. - Pressure-rise coefficient.



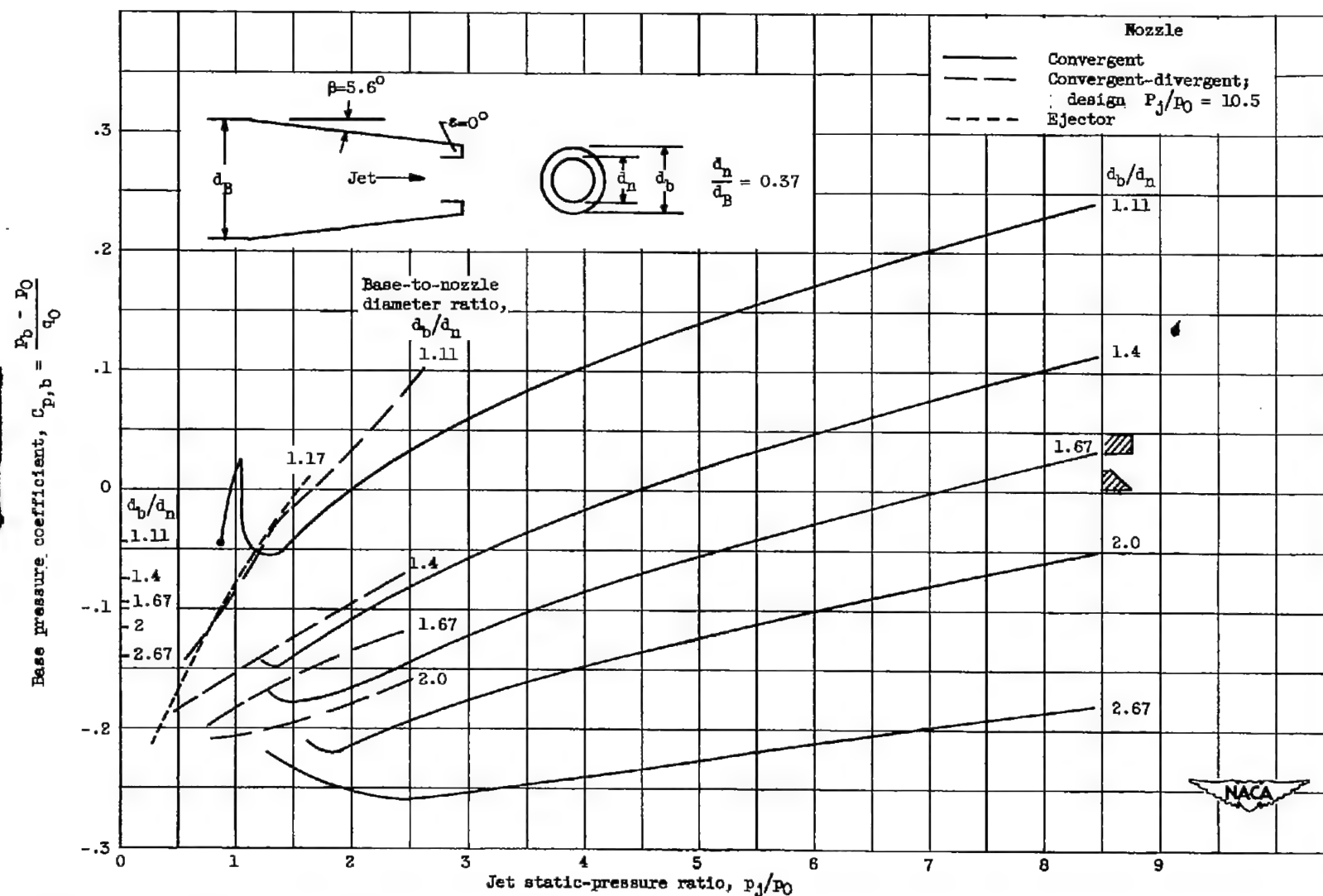


Figure 6. - Jet effects on base pressure. Free-stream Mach number, 1.9. (Base pressures with no jet flow indicated on ordinate.)

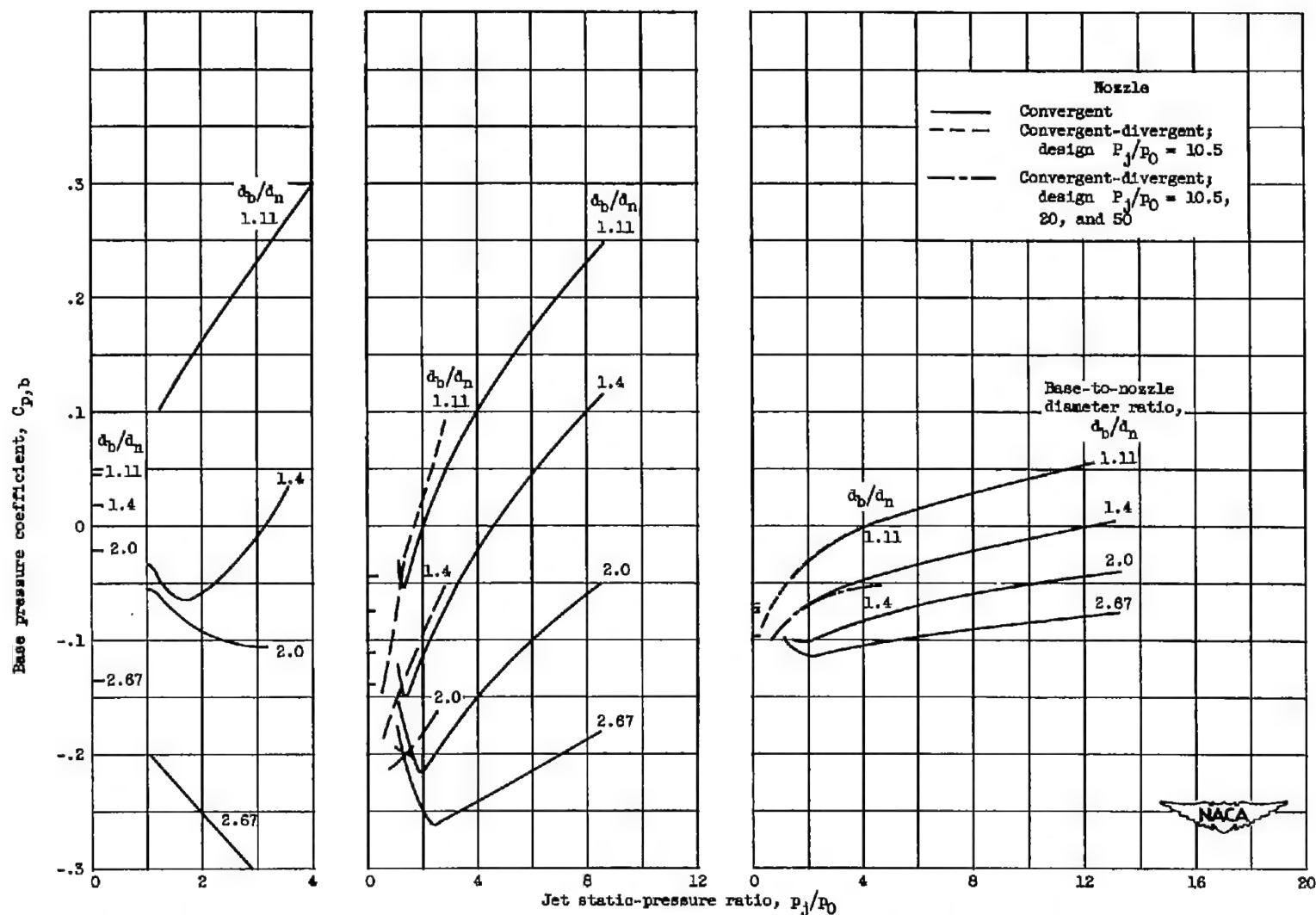


Figure 7. - Effect of free-stream Mach number. Boattail angle,  $5.6^\circ$ ; nozzle-to-body diameter ratio, 0.37. (Base pressures with no jet flow indicated on ordinate.)

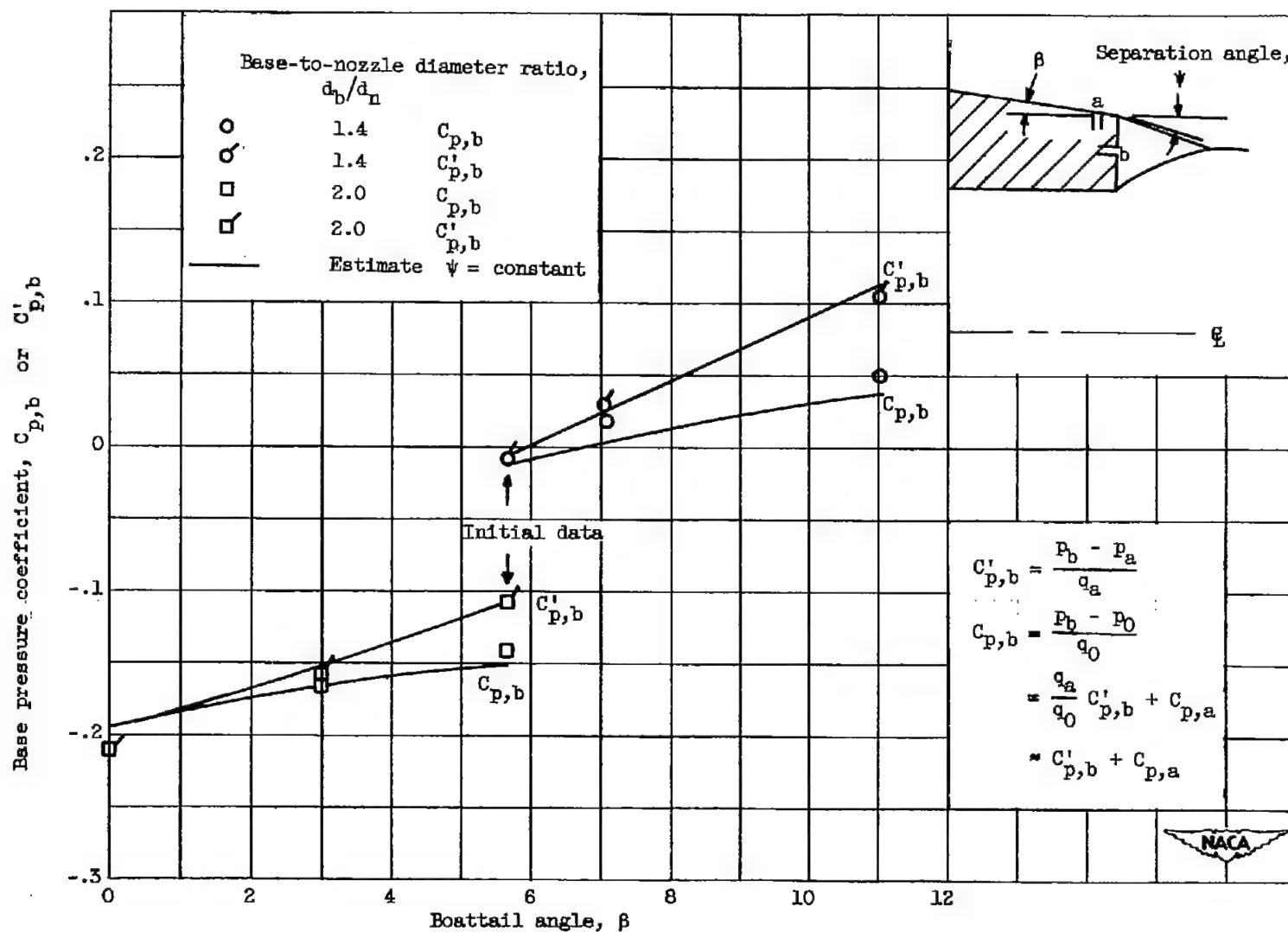


Figure 8. - Effect of afterbody geometry. Free-stream Mach number, 1.9; convergent nozzle; jet total-pressure ratio, 8.

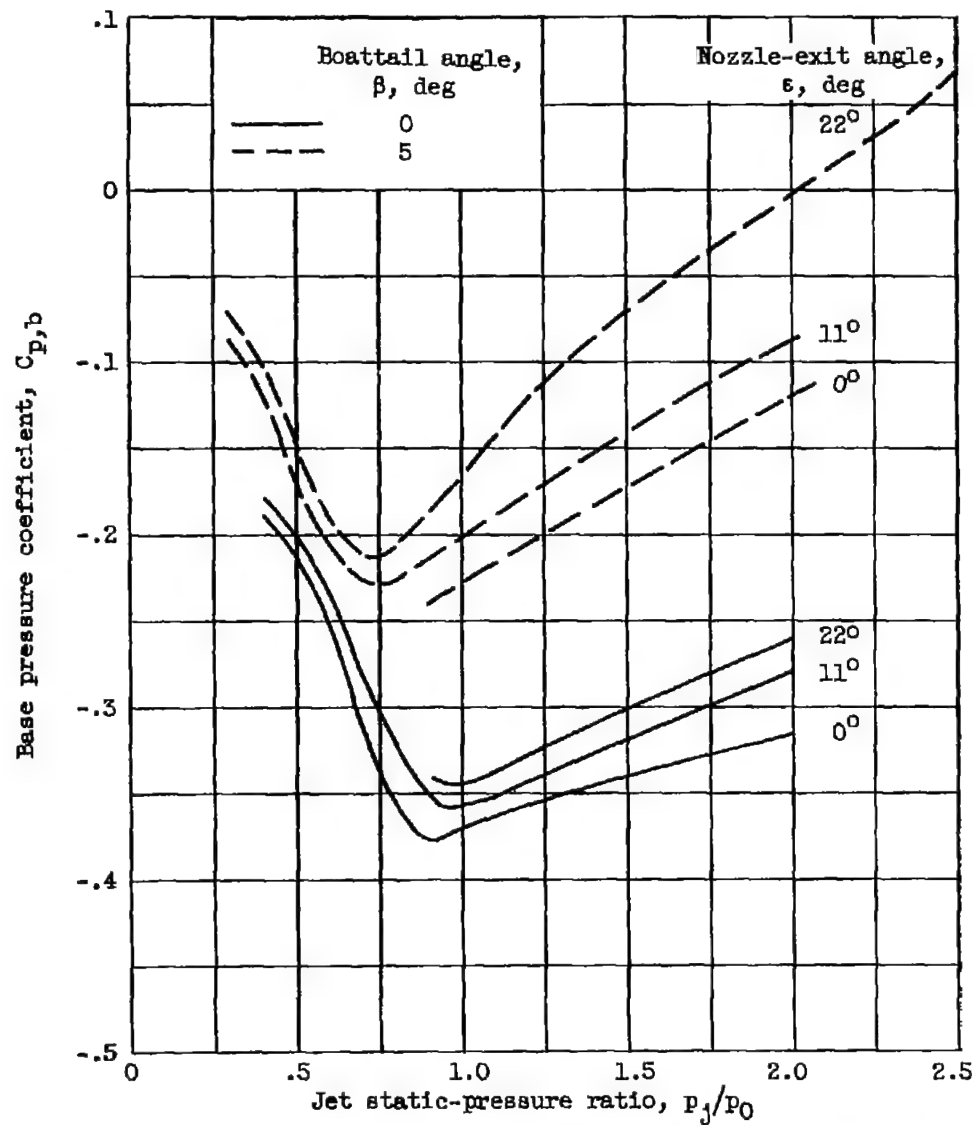
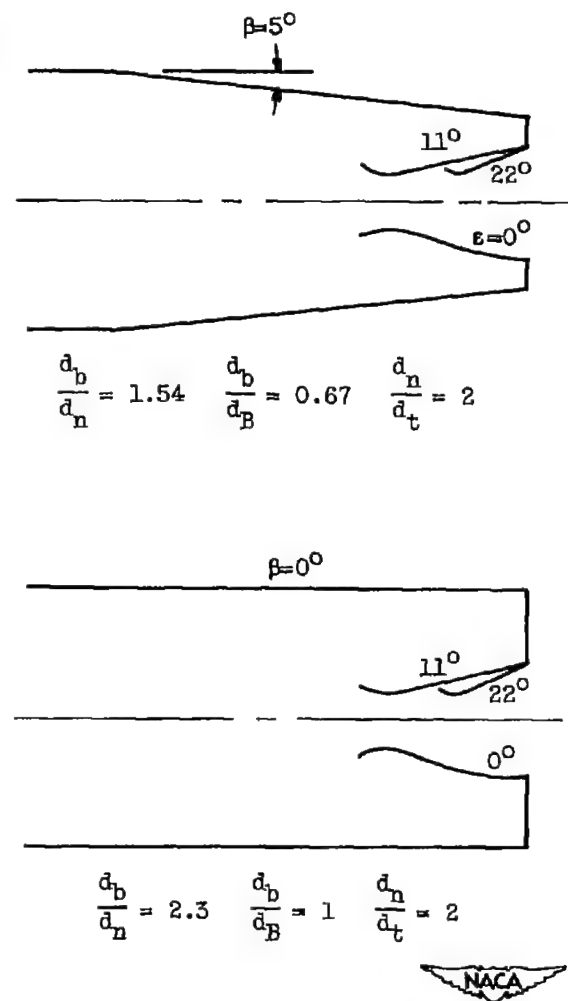
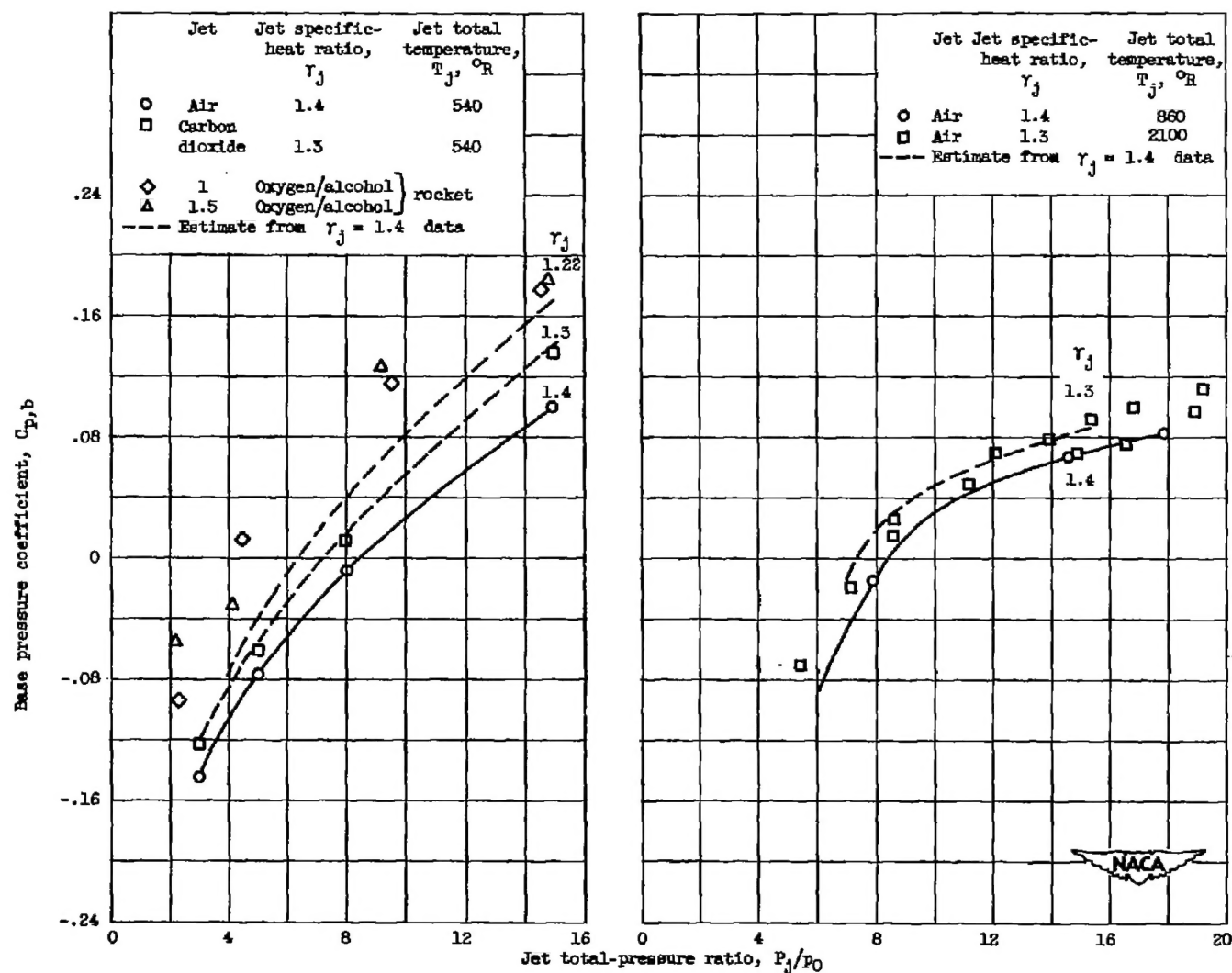


Figure 9. - Effect of nozzle-exit angle. Free-stream Mach number, 1.6.



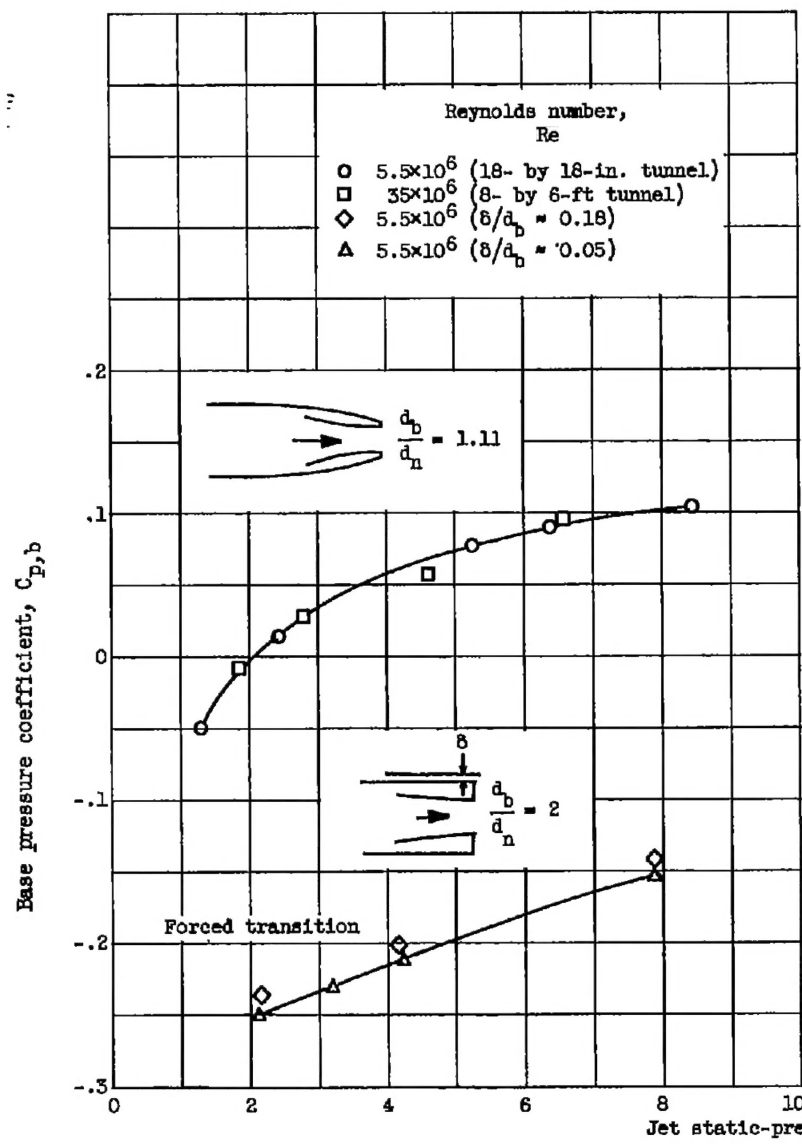
CONFIDENTIAL



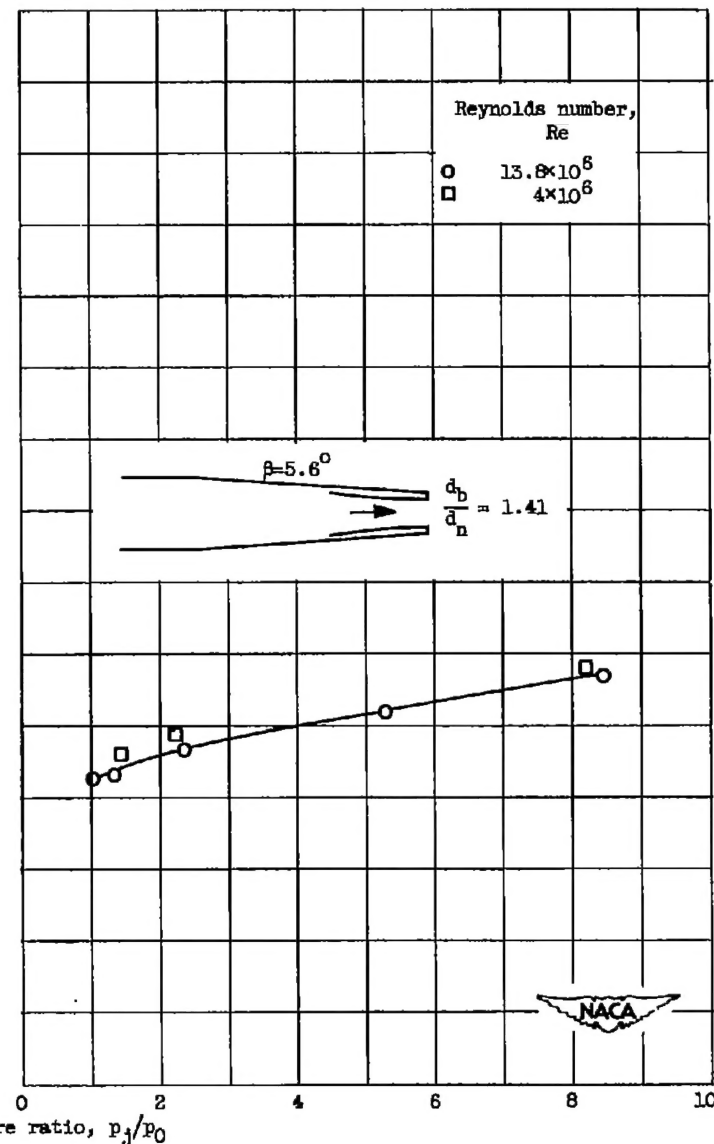
(a) 18- by 18-inch tunnel. Free-stream Mach number, 1.9; Reynolds number, approximately  $5.5 \times 10^6$ .

(b) 8- by 6-foot tunnel. Free-stream Mach number, 2.0; Reynolds number, approximately  $35 \times 10^6$ .

Figure 10. - Effect of jet temperature.

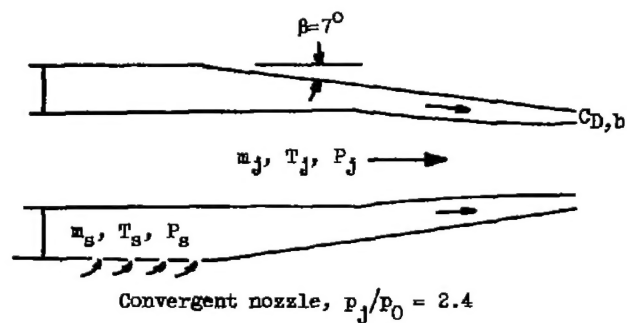


(a) Free-stream Mach number, 1.9 to 2.0.



(b) Free-stream Mach number, 3.1.

Figure 11. - Effect of Reynolds number with turbulent boundary layer ahead of base.



$$C_{D,b} = - \underset{1}{C_{p,b}} - \underset{2}{\frac{m_s V_s}{q_0 A_b}} + \underset{3}{\frac{m_s V_0}{q_0 A_b}}$$

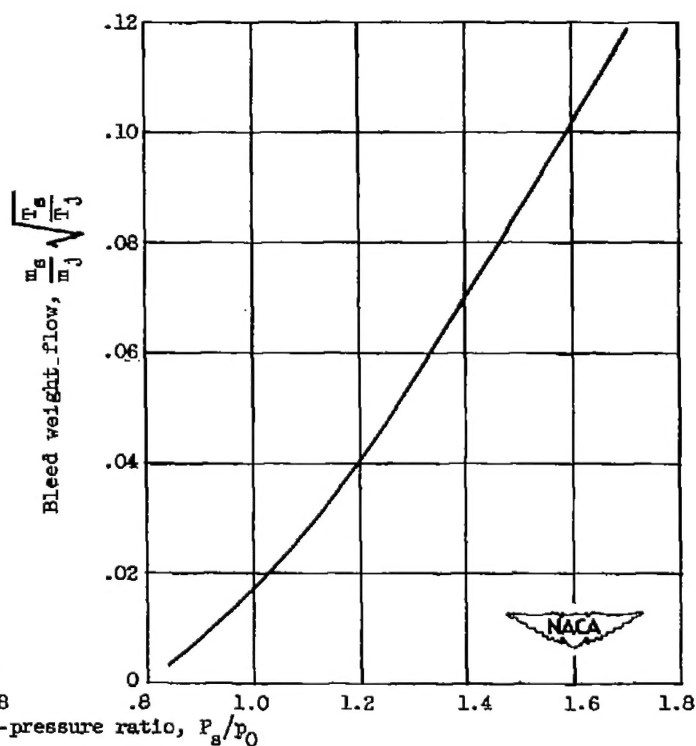
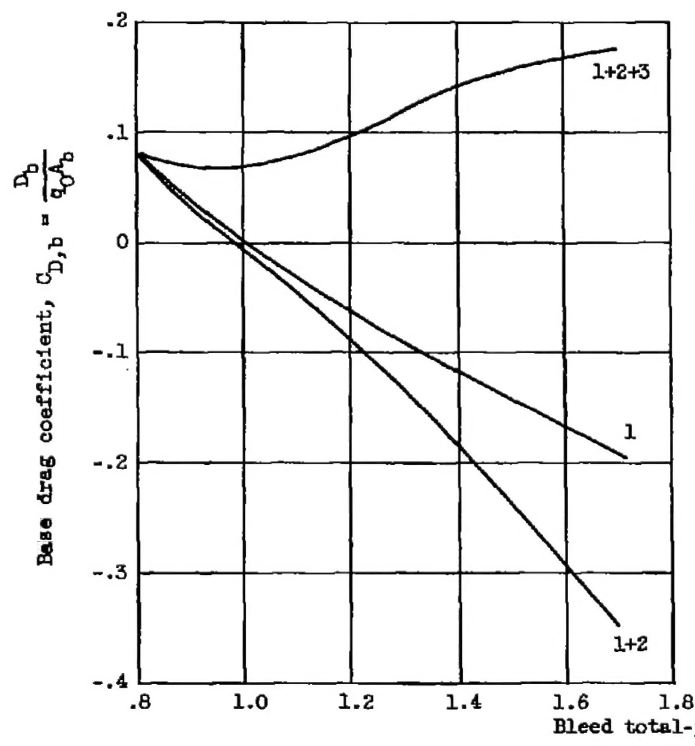
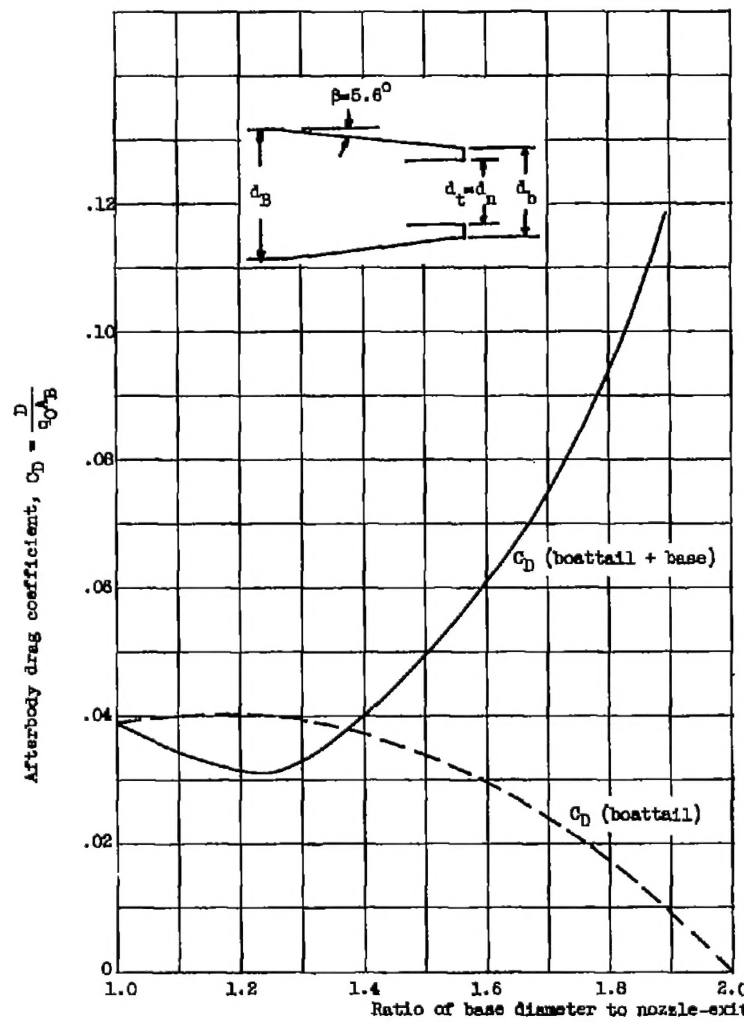


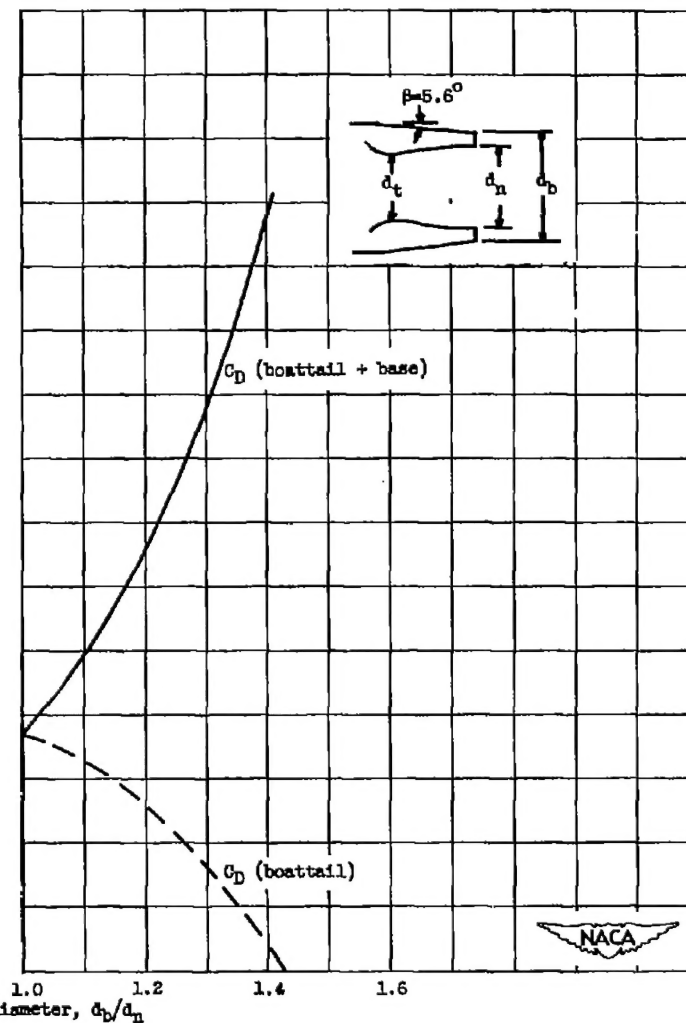
Figure 12. - Effect of annular base bleed at free-stream Mach number of 1.9.

CONFIDENTIAL

NACA RM E53E25



(a) Convergent nozzle; nozzle-to-body diameter ratio, 0.5.



(b) Convergent-divergent nozzle; nozzle-to-body diameter ratio, 0.7.

Figure 13. - Over-all afterbody drag considerations. Free-stream Mach number, 1.8; jet total-pressure ratio, 10; ratio of nozzle throat diameter to body diameter, 0.5.